Formation and Stability of a Nitric Oxide Donor: *S*-Nitroso-*N*-acetylpenicillamine

Itai Chipinda and Reuben H. Simoyi*

Department of Chemistry, Portland State University, Portland, Oregon 97207-0751

Received: June 9, 2005; In Final Form: January 6, 2006

The formation, reaction dynamics, and detailed kinetics and mechanism of the reaction between nitrous acid and *N*-acetylpenicillamine (NAP) to produce *S*-nitroso-*N*-acetylpenicillamine (SNAP) was studied in acidic medium. The nitrous acid was prepared in situ by the rapid reaction between sodium nitrite and hydrochloric acid. The reaction is first order in nitrite and NAP. It is also first order in acid in pH conditions at or slightly higher than the pK_a of nitrous acid. In lower pH conditions, the catalytic effect of acid quickly saturates. Higher acid concentrations also induce a faster decomposition rate of the SNAP, thus precluding the quantitative formation of SNAP from HNO_2 and NAP. Both HPLC and quadrupole time-of-flight mass spectrometry techniques proved that SNAP was the sole product produced. No nitrosation occurred on the secondary amine center in NAP, and only the thiol group reacted to form the nitrosothiol. Cu(I) ions were found to be effective SNAP-decomposition catalysts. Cu(II) ions had no effect on the stability of SNAP. Ambient oxygen in reaction solutions was found to have no effect on initial rates of formation of SNAP, products obtained, and stability of SNAP. The formation of SNAP occurs through two distinct pathways. One involves the direct reaction of NAP and HNO_2 to form SNAP and eliminate water, and the second pathway involved the initial formation of the nitrosyl cation, NO^+, which then nitrosates the thiol. The bimolecular rate constant for the reaction of NAP and HNO_2 was derived as 2.69 M^{-1} s^{-1}, while that of direct nitrosation by the nitrosyl cation was 3.00 $\times$ 10^4 M^{-1} s^{-1}. A simple reaction network made up of four reactions was found to be sufficient in simulating the formation kinetics and acid-induced decomposition of SNAP.

Introduction

It has become apparent since the early 1990s that nitric oxide (NO) has a crucial and extensive role in human physiology. NO, which is synthesized in vivo via the oxidation of L-arginine to citrulline by the enzyme NO synthase,[1] acts as a messenger molecule effecting muscle relaxation.[2] It is a cytotoxic agent in the nonspecific immune system,[3] a carcinogen,[4] and it also serves as a neurotransmitter in the brain and peripheral nervous system.[5] This small molecule is also known to inhibit platelet aggregation[6] and is involved in host defense,[7] among its other diverse physiological roles. The reaction of superoxide dismutase and hydrogen peroxide with NO is known to produce the peroxynitrite ion ($ONOO^-$), a major culprit in cell death.[8] Many research workers have come up with results and mechanistic propositions that are controversial and exhibit the complex biological roles of this simple molecule in the mammalian body. A number of reviews have tried to outline the physiological and pathophysiological roles of NO.[9,10]

NO has been administered orally in the form of organic nitrates for patients with ischaemic heart disease and other sources have been molecules such as sodium nitroprusside and diazeniumdiolates.[11] These NO donors fell out of favor, though, when evidence emerged that some patients developed tolerance to the organic nitrates which were used to administer NO.[12] Cyanide toxicity was a possibility in the case of nitroprussides[13] and little was known of the fate of diazeniumdiolates that were subsequently formed in the body.

S-Nitrosothiols with the general structure RSNO (where R is mainly an organic group) are an emerging class of both endogenous and exogenous NO donors. The existence of natural thiol containing proteins and peptides such as cysteine,[14,15] glutathione,[16] and albumin[17,18] and their nitrosation[19] leads us to believe that RSNOs are an endogenous reservoir of NO. The concentrations at which the RSNOs occur in vivo is debatable as efforts are still underway to develop methods for their detection. It has been reported that some of these thionitrites have been detected in the submicromolar range in plasma[20] and bronco-alveolar lavage fluid.[21] Degradation of these RSNOs enzymatically[22−26] or nonenzymatically[27−29] is believed to release the NO to target tissues where it will play its assigned physiological role. Despite the ease with which the biologically relevant thiols can be nitrosated in aqueous solutions[30,31] there seems to be a general lack of kinetics data and mechanistic understanding of how the *S*-nitrosothiols are formed.[32] There is need to probe the kinetics of the nitrosation[33,34] in vitro with the aim of linking these reactions with what actually transpires in the mammalian body. A detailed understanding of how the RSNOs are formed cannot be achieved without identifying and characterizing the products of the nitrosation reaction.[35] This has also been a neglected area of RSNO research work. In-depth understanding of the kinetics and mechanisms of thiol nitrosation as well as the stabilities of the nitrosothiols will contribute to the ongoing studies of these novel NO donors and shed light on the design of RSNOs with better pharmacokinetic properties. In this paper we report on the nitrosation of *N*-acetylpenicillamine with NO produced in situ through the acidification of sodium nitrite.

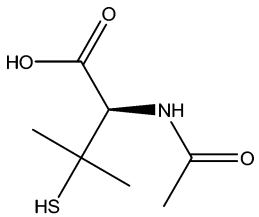

N-acetylpenicillamine

10.1021/jp0531107 CCC: $33.50
Published on Web 02/22/2006

Experimental Section

Materials. *N*-Acetyl-D-penicillamine (99%) (NAP), dimethyl sulfoxide (DMSO) (99.9% with 1% v/v TMS), *N*,*N*-dimethylaniline, EDTA, deuterated hydrochloric acid (99.8%) (Sigma-Aldrich), sodium nitrite, sodium chloride, and hydrochloric acid (Fisher) were used as purchased. Stock NAP and nitrite solutions were prepared just before use. Reagent solutions were prepared with distilled deionized water (Nanopure) from a Barnstead Sybron Corporation water purification unit.

Methods. All experiments were carried out at 25 ± 0.5 °C and at a constant ionic strength of 0.25 M (NaCl or $NaClO_4$). Although some experiments were run in sodium perchlorate, all experimental runs performed for the derivation of kinetics constants were run in NaCl. NaCl was preferred over $NaClO_4$ because HCl was the acid used in the formation of nitrous acid. Control experiments, utilizing either of these inert salts, showed no difference in overall reaction dynamical behavior. Inductively coupled plasma mass spectrometry (ICPMS) was utilized to quantify the concentrations of metal ions in the water used to prepare reagent solutions. ICPMS analysis showed negligible concentration of copper, iron, and silver (less than 0.1 ppb) and approximately 1.5 ppb of cadmium as the metal ion in highest concentrations. Control experiments were performed in distilled deionized water treated with the chelators EDTA or deferroxamine to establish the possible catalytic effects of adventitious metal ions. The reaction dynamics were mostly unaffected by the use of chelators (see the Results section for quantification of this effect in Figure 7B). The reaction system studied was essentially the HNO_2−NAP reaction. The progress of this reaction was monitored spectrophotometrically by following the absorbance of *S*-nitroso-*N*-acetyl-D-penicillamine (SNAP) at its experimentally determined absorption peak of 339 nm where an absorptivity coefficient of 890.5 M^{-1} cm^{-1} was evaluated. Product identification and verification was achieved by UV/vis spectrophotometry, ^1H NMR spectrometry, HPLC, and quadrupole time-of-flight mass spectrometry. Kinetics measurements for fast reactions were performed with the Hi-Tech Scientific double-mixing SF61-DX2 stopped-flow spectrophotometer. Slower reactions and absorbance readings were performed on a Perkin-Elmer Lambda 2S UV/vis spectrophotometer.

Stoichiometric determinations were performed by varying NO_2^- and keeping both NAP and acid constant and testing for the presence of any remaining NO_2^- as the nitrous acid (HNO_2). The presence of NO_2^- was quantitatively analyzed (gravimetrically) as the orange chloride salt of *p*-nitroso-*N*,*N*-dimethylaniline that was formed when the solution was reacted with *N*,*N*-dimethylaniline. Reaction was guaranteed to proceed to completion by maintaining both acid and nitrite in excess over NAP. Due to the well-known decomposition of nitrosothiols, product reaction solutions were not allowed to stand for more than an hour before the addition of *N*,*N*-dimethylaniline. The salt formed, however, was allowed to settle for 24 h before being filtered, dried, and weighed.

^1H NMR Techniques. Structural characterization of the SNAP formed was done with a Varian 500 MHz ^1H NMR spectrometer, using dimethyl sulfoxide (DMSO) adulterated with TMS. DCl was used for pH adjustment.

The HPLC Technique. The HPLC system utilized a Shimadzu (Columbia, MD) SPD-M10A VP diode array detector, dual LC-600 pumps, LPT-6B LC-PC Interface controller, SIL-10AD auto injector, and Class-VP Chromatography Data System software. All samples were loaded on a reverse phase Discovery 5 μm C_{18} HPLC column (Supelco, Bellefonte, PA). They were run isocratically at 5% acetonitrile/H_2O and all eluents were detected at a UV absorbance of 339 nm (for selective scans) with the maximum spectral scan mode employed to detect all eluents. A flow rate of 1 mL/min was maintained. All solutions for HPLC analysis were made with Milli-Q Millipore purified water and filtered with Whatman Polypropylene 0.45 μm pore-size filter devices before injection (10 μL) into the column using the auto injector. To curb the interaction of the protonated amines on the analytes with the silanol groups on the stationary phase (which was causing tailing of the peaks) the sodium salt of 1-octanesulfonic acid (0.005 M) was incorporated into the aqueous mobile phase. This was sufficient to neutralize the protonated amines and produce good resolution while eliminating peak tailing.

Time-of-Flight Mass Spectrometry. Mass spectra were acquired on a Micromass QTOF-II (Waters Corporation, Millford, MA) quadrupole time-of-flight mass spectrometer. Analytes were dissolved in 50/50 acetonitrile/water, and analyte ions were generated by positive-mode electrospray ionization (ESI)[1] at a capillary voltage of 3.5 kV and a flow rate of 5 μL/min. The source block was maintained at 80 °C and the nitrogen desolvation gas was maintained at 150 °C and a flow rate of 400 L/h. Tandem mass spectrometry (MS/MS) data were generated via collision-induced dissociation (CID) on argon with a collision energy of 10−20 eV. Data were visualized and analyzed with the Micromass MassLynx 4.0 software suite for Windows 2000 (Waters Corporation, Millford, MA).

Synthesis of SNAP. To a stirred ice cold solution of NAP (0.478 g, 25 mmol) in 8.0 mL of water containing 2.5 mL of 1.0 M HCl was added (0.173 g, 25 mmol) $NaNO_2$. After 40 min at 5 °C the solution was treated with 5 mL of acetone and stirred for a further 10 min. The green precipitate was filtered off with vacuum filtration and washed 5 times with ice cold water and 3 times with 10 mL aliquots of acetone and diethyl ether. The precipitate was left to dry out before a mass spectrometer analysis could be done. The synthesized SNAP was utilized to derive a standard UV spectrum from which a standard absorptivity coefficient could be calculated.

Results

The stoichiometry of the reaction involved the reaction of 1 mol of NAP with 1 mol of nitrous acid to produce 1 mol of SNAP accompanied by elimination of a water molecule and with reaction occurring solely at the thiol center:

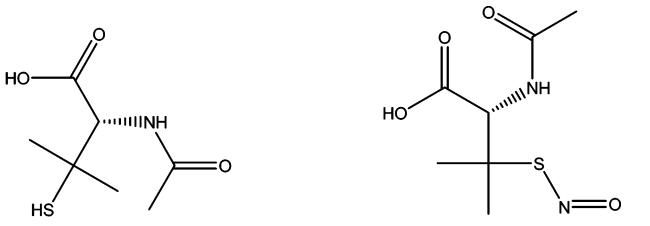

N-acetyl-D-penicillamine + HNO_2 → S-nitroso-N-acetyl-D-penicillamine + H_2O (R1)

The stoichiometry was derived by the use of several complementary techniques. The SNAP synthesized in our laboratory was carefully weighed and its UV spectra obtained and compared with that from a commercially available sample. This spectrum is shown in Figure 1A with a peak at 338.5 nm and an absorptivity coefficient of 890.5 M^{-1} cm^{-1}. For all our experimental data acquisitions, however, a λ_{max} of 339 nm with an absorptivity coefficient of 890 M^{-1} cm^{-1} was used. Reactions run for the deduction of the stoichiometry were set up with $[H^+]_0$, $[NO_2^-]_0 \gg [NAP]_0$ such that NAP was the limiting

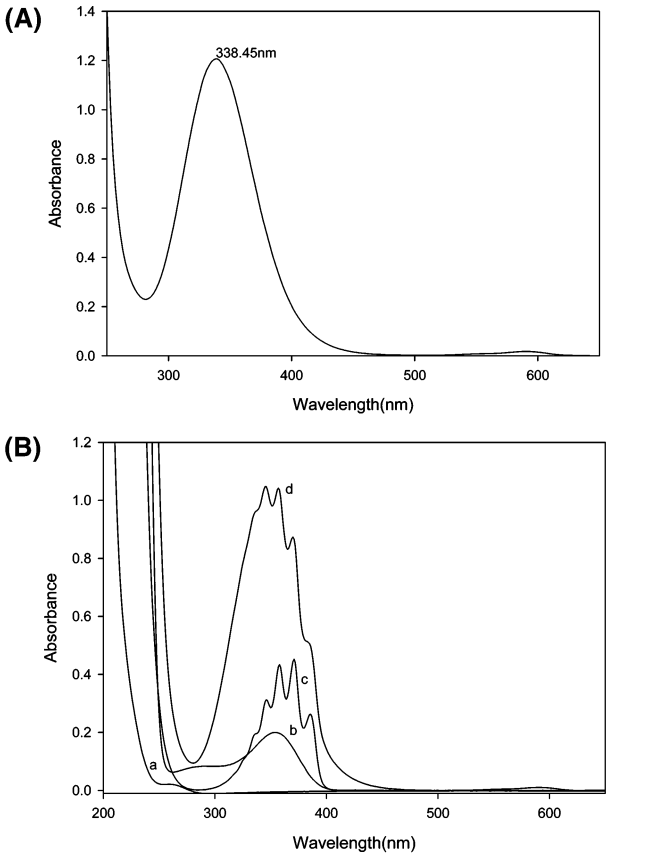

Figure 1. (a) UV/vis spectrum of a 1.35×10^{-3} M standard *S*-nitroso-*N*-acetylpenicillamine at neutral pH. Only one peak is available in the near-UV at 339 nm with an absorptivity coefficient of 890 M^{-1} cm^{-1}. (b) UV/vis spectral scans of reactants NAP (a), nitrite (b), nitrous acid (c), and product SNAP (d). The structure seen in the spectrum of SNAP is due to contribution from HNO_2 which, at these conditions, was in excess. The overall absorbance observed at 339 nm is higher than the expected 0.890 because of contributions from nitrite and nitrous acid.

reagent. The reaction was allowed to proceed to completion while rapidly scanning the reaction solution between 250 and 450 nm. The maximum absorbance obtained at 339 nm was noted and the concentration of SNAP was deduced from this maximum absorption. Typical reaction times were in the range of 5−15 min. Further incubation of the reaction solutions showed a decrease in the peak at 339 nm as the nitrosothiol slowly released the nitric oxide and formed a disulfide (here SNAP is written as RSNO):[36]

$$2\mathrm{RSNO} \rightarrow \mathrm{RSSR} + 2\mathrm{NO} \qquad \text{(R2)}$$

In the physiological environment, the half-life for reaction R2 is approximately 10 h, and did not interfere with the kinetics of reaction R1. Typical spectra of reactants and products are shown superimposed in Figure 1B. The product solution resulting from excess acid and nitrite is shown as spectrum a. It differs from that shown in Figure 1A because of contribution from HNO_2 whose spectrum is shown in Figure 1B as spectrum b. Nitrite (spectrum c) also absorbs at 339 nm. The true absorption derived solely from SNAP was obtained after subtracting contributions from nitrite and HNO_2. In high enough acid conditions the expected spectrum and absorptivity coefficient could be obtained by assuming that all excess nitrite is in the form of nitrous acid. ^{1}H NMR spectra of NAP and SNAP were very similar, showing that the carbon skeleton of NAP was not disturbed by the nitrosation.

Figure 2A shows the HPLC spectral data that were used to confirm that SNAP is the sole product obtained from the reaction of nitrous acid and NAP. Spectrum (i) shows the spectrum obtained from the reaction mixture ($\mathrm{NAP} + \mathrm{NO_2^-} + \mathrm{H^+}$) which shows a peak after 4.9 min while spectrum (ii) is from standard SNAP and spectrum (iii) is from a combination of SNAP, NAP, and acid. On superimposing all three spectra in (iv), one can confirm that our reaction mixture only produces SNAP. The slight deviation obtained in the appearance of the peak of standard SNAP and the peak observed from the reaction mixture is attributable to the excess acid in the reaction mixture. This explains why peaks for spectra (i) and (iii) coincide exactly. The concentrations utilized in all three spectra were deliberately made unequal so that each peak could be clearly resolved in the superimposed spectra (iv).

The time-of-flight mass spectra from the reaction product and synthesized standard SNAP are shown in Figure 2B,C. These two compounds give nearly identical spectra. The *m*/*z* 191.06 peak is from the thiol molecule, NAP. In the reaction product this peak appears on *m*/*z* 192.06 due to protonation of the nitrogen or thiol groups which occur in the excess acid conditions that were employed in producing this product solution:

$$\mathrm{NAP} + \mathrm{H^+} \rightleftharpoons [\mathrm{NAP{-}H}]^+ \qquad \text{(R3)}$$

The first protonation would occur at the secondary amine center, which is slightly more basic than the thiol center. The SNAP, in both spectra in Figure 2B, appear at *m*/*z* 221.06. The MSMS fragmentation patterns of the *m*/*z* 221.06 peak in both cases are also nearly identical (Figure 2C, (i) and (ii)). The most important deduction from the QTOF spectra is the absence of any product from the possible nitrosation of the secondary amine in NAP. This is a well-known reaction in which nitrous acid reacts with a secondary amine to yield an *N*-nitrosoamine:

$$\mathrm{R_1R_2NH} + \mathrm{HNO_2} \rightarrow \mathrm{R_1R_2N{-}N{=}O} + \mathrm{H_2O} \qquad \text{(R4)}$$

It appears that under the conditions in which the kinetics of formation of SNAP were studied, formation of the nitrosoamine is negligible.

Oxygen Effects. Molecular oxygen is known to be an important reagent in many reactions involving sulfur compounds. It is also known to interfere in many reactions involving oxides of nitrogen. Nitric oxide autoxidizes in aerobic environments to yield predominantly nitrogen dioxide and other nitrogen oxides.

$$2\mathrm{NO} + \mathrm{O_2} \rightarrow 2\mathrm{NO_2} \qquad \text{(R5a)}$$

$$\mathrm{NO} + \mathrm{NO_2} \rightarrow \mathrm{N_2O_3} \qquad \text{(R5b)}$$

$$\mathrm{N_2O_3} + \mathrm{H_2O} \rightarrow \mathrm{NO_2^-} + \mathrm{H^+} \qquad \text{(R5c)}$$

Aerobic environments also encourage the formation of peroxynitrite anions from the reaction of superoxide radical anion with nitric oxide.[37]

$$\mathrm{NO} + \mathrm{O_2^{\bullet -}} \rightarrow \mathrm{ONOO^-} \qquad \text{(R6)}$$

Thiols represent preferential targets of the peroxynitrite anion in biological systems.[38] Peroxynitrites oxidize thiols to the dimeric disulfides. Reaction R6, however, is more viable in basic environments. Most of the kinetics data presented in this paper were obtained in low pH environment, thus rendering reaction R6 less effective under our reaction conditions. At room

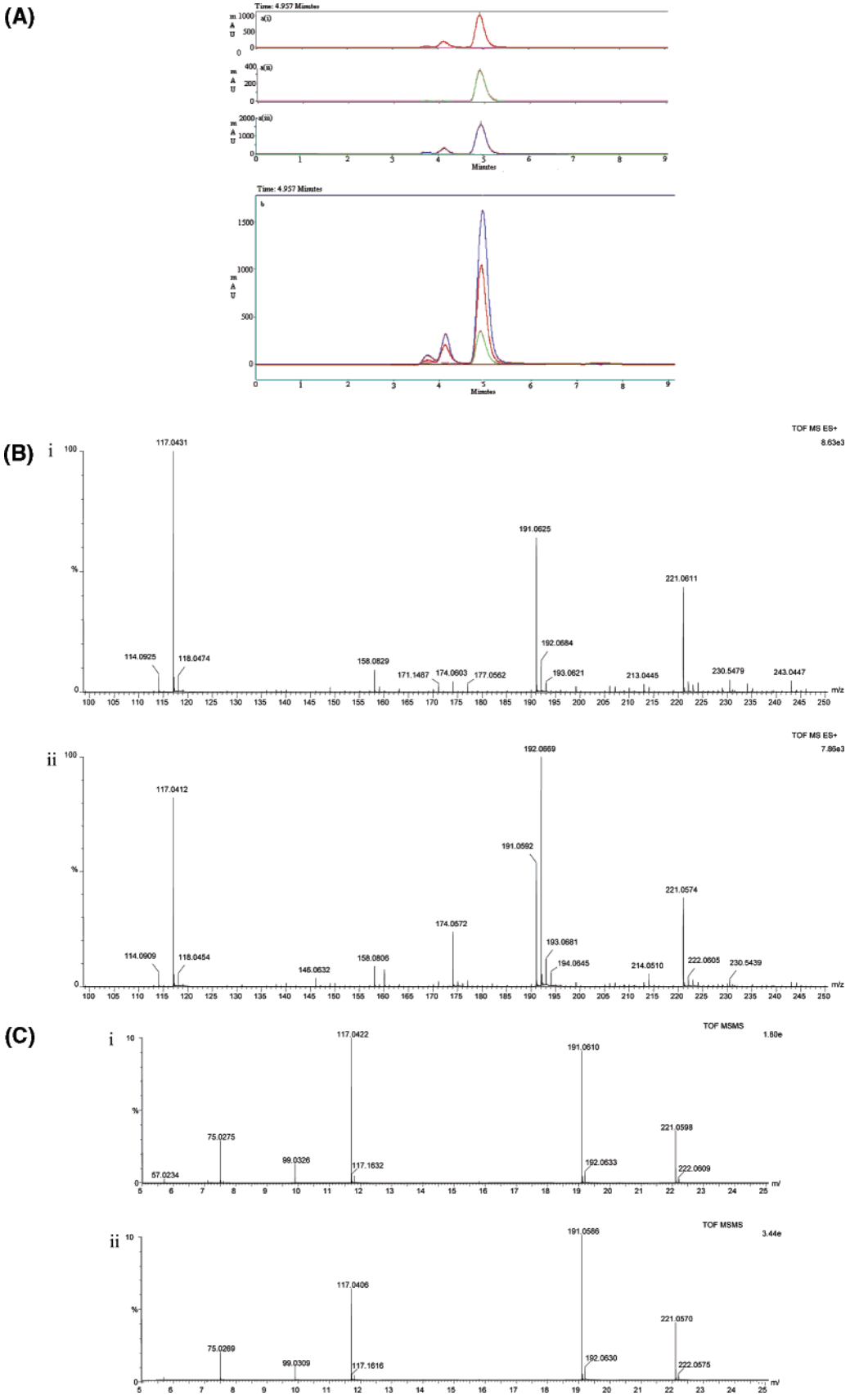

Figure 2. (A) Product confirmation of the nitrosation reaction: (a(i)) 8.334 mM NAP + 4.167 mM HNO_2 + 25 mM H^+; (a(ii)) 1.135 mM SNAP standard + 25 mM H^+; and (a(iii)) co-injection of 1.135 mM SNAP standard + 8.334 mM NAP + 4.167 mM HNO_2 + 25 mM H^+. (b) Overlay of the spectra in part a. The appearance of the single peak at 5 min for part C confirms the product to be SNAP. (B) Comparison of the standard nitrosothiol and the reaction product: (i) 4.54×10^{-7} M SNAP standard in acetonitrile/H_2O and (ii) 4.540×10^{-7} M of reaction product in acetonitrile/H_2O. (C) The standard nitrosothiol and the reaction product gave the same fragmentation pattern when MSMS fragmentation was done on the parent peak, m/z =221.0570: (i) SNAP standard and (ii) reaction product.

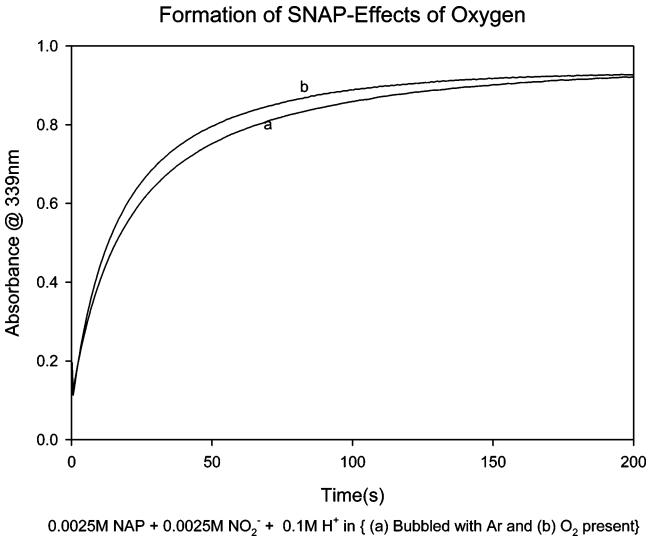

Figure 3. Effect of oxygen on the nitrosation of NAP. Neither initial rates nor the final amount of SNAP formed are altered by the presence of oxygen.

temperature and pressure aqueous solutions are 0.2 mM in oxygen in neutral pH conditions, and at such low concentrations, reaction R5a would be too slow to be competitive. Figure 3 shows two reaction traces at identical initial conditions in which one solution was ultrasonicated and degassed with argon. The final absorbances in both experiments were identical, and initial rates were also identical. The two traces only differed in the middle part of the reaction, which was not utilized for kinetics measurements and stoichiometric determinations. Thus, in most of our experiments, ambient dissolved oxygen concentrations were not controlled.

Reaction Kinetics. The reaction involved the nitrosation of NAP by nitrous acid. The nitrous acid was prepared in situ by the acidification of sodium nitrite. The stopped-flow configuration involved the mixing of NAP, acid, and chloride or sodium perchlorate in one feed stream, with the other feed stream containing solely sodium nitrite. The injection of acid and nitrite into separate feed streams precluded the possibility of the nitrous acid decomposing before nitrosation commenced. Most reactions were run with NAP as the limiting reagent. Figure 4A shows the effect of varying NAP concentrations at constant acid and nitrite concentrations. Initial rate plots with respect to NAP concentrations show a linear plot with an intercept kinetically indistinguishable from zero. The reaction showed a first order dependence in NAP over a wide range of NAP concentrations for as long as $[NO_2^-]_0$, $[H^+]_0 > [NAP]_0$. Figure 4C shows the same traces as in Figure 4A at higher acid concentrations. At these acid concentrations the reaction went to completion (producing the expected maximum SNAP as per stoichiometry R1) within 20 s. All NAP introduced into the reaction mixture was quantitatively converted to SNAP. If observation of the traces in Figure 4C was continued further, a slow decrease in concentration of SNAP was next observed. This is expected since nitrosothiols are known to be nitric oxide donors. At the concentrations utilized for Figures 4A−C the rate of formation of SNAP is much faster than its decomposition rate.

The effect of varying nitrite is shown in Figure 5A. The amount of SNAP formed increases until the nitrite concentrations exceed NAP concentrations and a saturation is attained. The final absorbances observed, however, continue to increase after nitrite concentrations exceed NAP concentrations because of the contribution to the absorbance observed at 339 nm from nitrite and HNO_2. Absorbance from SNAP is obtained by

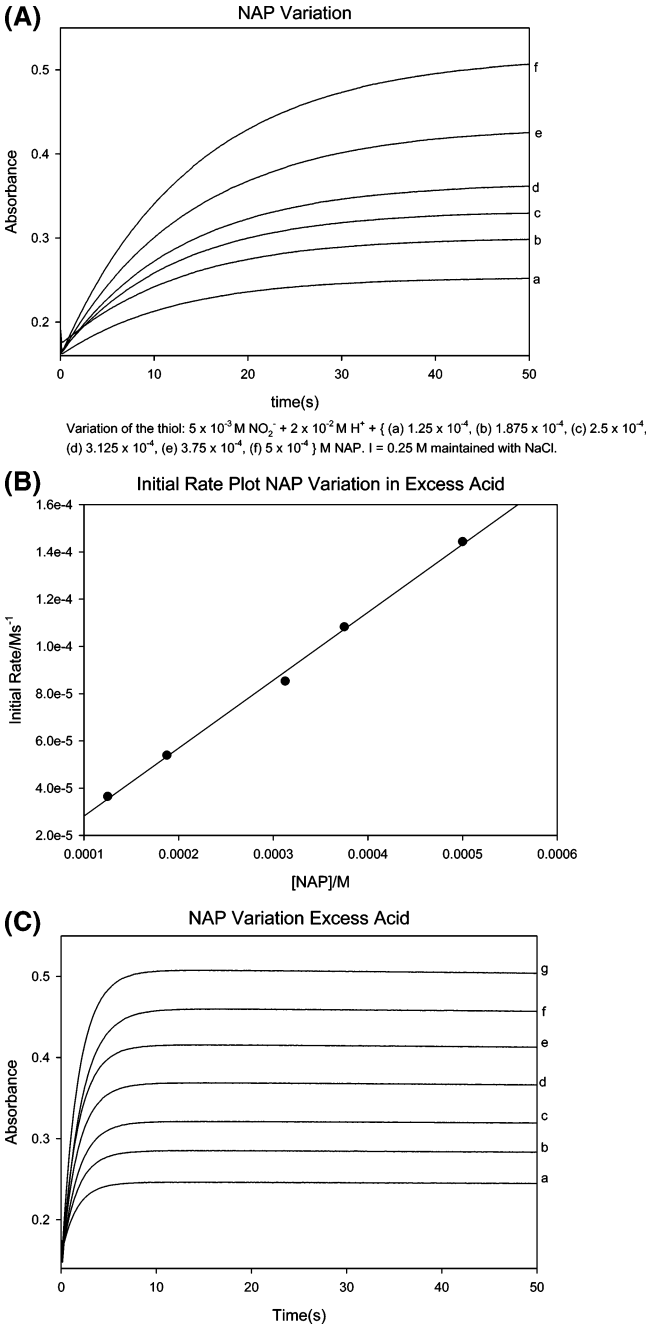

Figure 4. (A) Absorbance traces showing the effect of varying NAP concentrations. The reaction shows first-order kinetics in NAP. $[NO_2^-]_0 = 5 \times 10^{-3}$ M; $[H^+]_0 = 2.0 \times 10^{-2}$ M; $[NAP]_0 =$ (a) 1.25×10^{-4}, (b) 1.88×10^{-4}, (c) 2.5×10^{-4}, (d) 3.125×10^{-4}, (e) 3.75×10^{-4}, and (f) 5.0×10^{-4} M. (B) Initial rate plot of the data in part A. The intercept is small enough to be kinetically indistinguishable from zero. The plot shows the strong first-order dependence of the rate of formation of SNAP on NAP. (C) The same NAP dependence traces performed at higher acid concentrations to those shown in part A. The quantitative production of SNAP occurs much earlier in high acid conditions. $[NO_2^-]_0 = 5 \times 10^{-3}$ M; $[H^+]_0 = 4.0 \times 10^{-2}$ M; $[NAP]_0 =$ (a) 1.25×10^{-4}, (b) 1.88×10^{-4}, (c) 2.5×10^{-4}, (d) 3.125×10^{-4}, (e) 3.75×10^{-4}, (f) 5.0×10^{-4}, and (g) 6.0×10^{-4} M.

subtracting the contributions from these two species. Figure 5B also shows that the rate of formation of SNAP is first order in nitrite concentrations.

Kinetics of formation of SNAP has a more complex dependence on acid. Figure 6A shows acid variations which show that at high enough acid concentrations the decomposition of SNAP occurs before its quantitative formation is complete. The

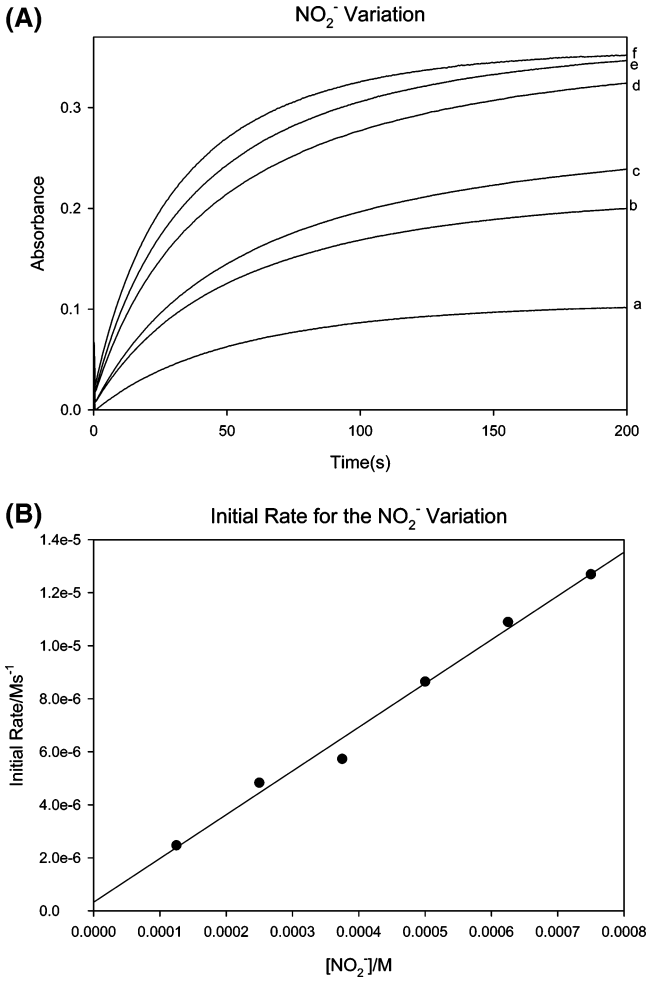

Figure 5. (A) The effect of varying nitrite concentrations. Traces a−c have less than stoichiometric amounts of nitrite. Trace d has the 1:1 stoichiometric ratio of NAP to nitrite. $[NAP]_0 = 5.0 \times 10^{-4}$ M; $[H^+]_0 = 0.04$ M; $[NO_2^-]_0 =$ (a) 1.25×10^{-4}, (b) 2.5×10^{-4}, (c) 3.75×10^{-4}, (d) 5.0×10^{-4}, (e) 6.25×10^{-4}, and (f) 7.5×10^{-4} M. (B) Initial rate plot of the data shown in part A. The formation of SNAP shows first-order kinetics in nitrite concentrations.

decomposition of SNAP can be delayed by the use of lower acid concentrations and by having excess nitrite and acid. Figure 6B shows the absorbance traces obtained in low acid conditions in which acid is less than nitrite concentrations and its concentration is progressively increased to when it is now slightly higher than that of nitrite. The acid dependence plot shown in Figure 6C appears discontinuous. With acid concentrations less than nitrite concentrations, the rate of formation of SNAP is first order with respect to nitrite. This plot also gives the expected intercept of a vanishing rate of reaction with zero nitrite concentrations. The plot, however, changes slope and loses linearity as soon as acid concentrations exceed that of nitrite. This would suggest a simple one-term rate law at low acid and a more complex multiterm rate law with respect to acid at higher concentrations.

Effect of Cu(I) and Cu(II) Ions. Cu(I) and Cu(II) ions are known to affect many reactions involving sulfur compounds. Figure 7A shows a series of experiments with varying amounts of Cu(I) ions. It shows a decrease in rate as well as a decrease in amount of SNAP obtained with increase in Cu(I) ions. It would appear that Cu(I) ions sequester some of the NAP molecules and makes them unavailable for further reaction due to the linear response of the amount of SNAP formed to the amount of Cu(I) ions added. A plot of $[Cu(I)]_0$ vs absorbance

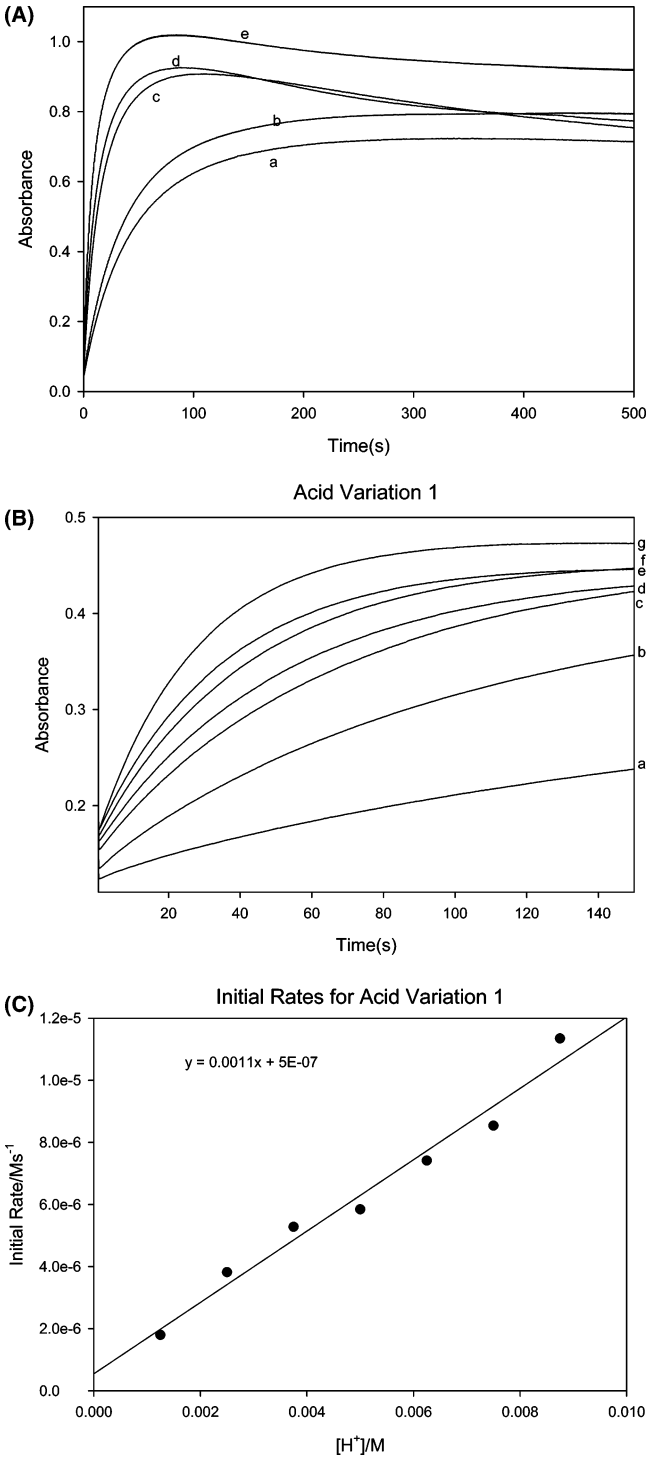

Figure 6. (A). Effect of medium to high acid concentrations on the formation of SNAP. High acid concentrations give an early onset of the decomposition of SNAP while also catalyzing formation of SNAP. $[NAP]_0 = 2.5 \times 10^{-4}$ M; $[NO_2^-]_0 = 2.5 \times 10^{-4}$ M; $[H^+]_0 =$ (a) 0.01, (b) 0.02, (c) 0.03, (d) 0.04, and (e) 0.05 M. (B) Effect of acid at low acid concentrations. There is a linear dependence on the rate of formation of SNAP at low acid concentrations. $[NAP]_0 = 2.5 \times 10^{-4}$ M; $[NO_2^-]_0 = 5.0 \times 10^{-3}$ M; $[H^+]_0 =$ (a) 1.25×10^{-3}, (b) 2.5×10^{-3}, (c) 5.0×10^{-3}, (d) 6.25×10^{-3}, (e) 7.5×10^{-3}, (f) 8.75×10^{-3}, and (g) 1.0×10^{-2} M. (C) Initial rate plots showing linear dependence of rate of reaction on acid at low acid concentrations. This plot is derived from data in part B.

due to SNAP was linear with a negative slope. The absorbance due to SNAP had to be calculated by subtracting the absorbance due to HNO_2 (see Figure 1B), and hence this linearity would

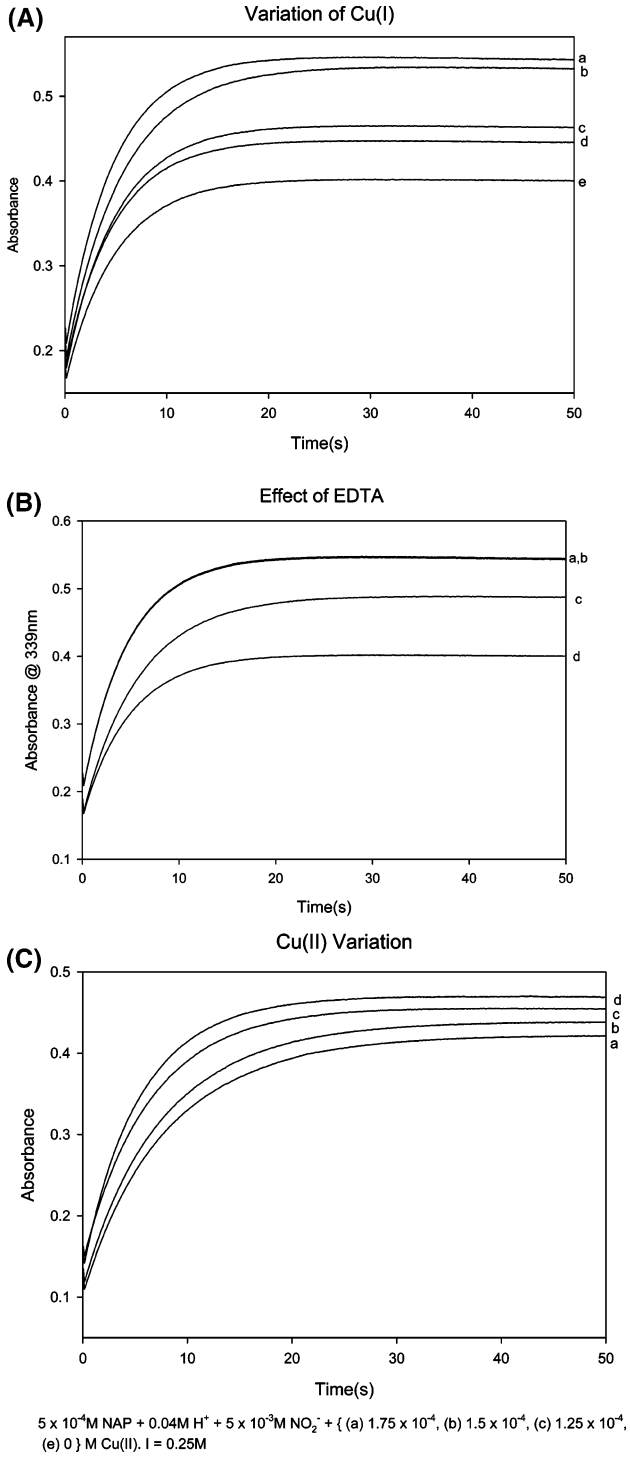

Figure 7. (A) Effect of Cu(I) on SNAP formation. There is a monotonic decrease in SNAP formation with increase in Cu(I) concentration. $[NAP]_0 = 5.0 \times 10^{-4}$ M; $[NO_2^-]_0 = 5.0 \times 10^{-3}$ M; $[H^+]_0 = 0.04$ M. $[Cu(I)]_0 =$ (a) 0, (b) 5.0×10^{-5}, (c) 7.5×10^{-5}, (d) 1.0×10^{-4}, and (e) 1.5×10^{-4} M. (B) Evaluating effect of Cu(I) by the use of metal ion chelators, EDTA. All experimental traces have $[NAP]_0 = 5.0 \times 10^{-4}$ M, $[NO_2^-]_0 = 5.0 \times 10^{-3}$ M, and $[H^+]_0 = 0.04$ M. Trace a is the control. Trace b has 0.0001 M EDTA. No difference is discernible between traces a and b, indicating that the water used for preparing reagent solutions did not contain enough trace metal ions to affect the kinetics. Trace c has 0.0001 M EDTA and 0.00015 M Cu(I) ions. Trace d is the same as trace c without the EDTA. (C) Effect of Cu(II) ions on the rate of formation of SNAP. All traces contained $[NAP]_0 = 5.0 \times 10^{-4}$ M, $[NO_2^-]_0 = 5.0 \times 10^{-3}$ M, and $[H^+]_0 = 0.04$ M. The other traces have the following Cu(II) ion concentrations: (a) 1.75×10^{-4}, (b) 1.5×10^{-4}, (c) 1.25×10^{-4}, (d) 1.0×10^{-4}, and (e) 0 M.

not be evident just by looking at Figure 7A. Figure 7B is a control experiment carried out to isolate the effect of Cu(I) ions. Trace a in Figure 7B represents a normal experimental run without copper ions. Trace b has the same initial conditions as trace a, but with a metal ion chelator, EDTA. There is a very small difference between the two traces, showing that the water supply used for the preparation of reagent solutions did not contain enough metal ions to affect the reaction dynamics and kinetics. Trace c has Cu(I) ions with EDTA. The concentrations of Cu(I) ions used in this trace were higher than the EDTA concentrations, thus ensuring that some Cu(I) would be free and not sequestered. This shows depletion of SNAP formed is proportional to the concentrations of the Cu(I) ions that were not sequestered. The EDTA is completely removed in trace d and the result is a lower formation of SNAP. Figure 7C shows a series of experiments with Cu(II) ions. They give the reverse of the effects of Cu(I) ions. Their inclusion gives a complex that contributes to the absorbance at 339 nm. The initial rates of formation of SNAP, however, are not altered by addition of Cu(II).

Mechanism

The reaction dynamics suggest only four reactions as being relevant in the production of SNAP. They involve the protonation of nitrite to produce nitrous acid followed by the production of the nitrosyl ion[39] and the reaction of both nitrous acid and nitrosyl cation with NAP. Since the only chemical reactivity during nitrosation is occurring at the thiol center of NAP, for the purposes of this mechanism, we denote NAP as the generic thiol, RSH.

$$H^+ + NO_2^- \rightleftharpoons HNO_2 \qquad k_1, k_{-1}; K_a^{-1} \qquad \text{(R7)}$$

$$HNO_2 + H^+ \rightleftharpoons {}^+N{=}O + H_2O \qquad k_2, k_{-2} \qquad \text{(R8)}$$

$$RSH + HNO_2 \rightarrow RSNO + H_2O \qquad k_3 \qquad \text{(R9)}$$

$$RSH + {}^+N{=}O \rightleftharpoons RSNO + H^+ \qquad k_4, k_{-4} \qquad \text{(R10)}$$

The rate of reaction, based on the formation of RSNO, is given by:

$$d[SNAP]/dt = k_3[RSH][HNO_2] + k_4[RSH][{}^+N{=}O] - k_{-4}[SNAP][H^+] \quad (1)$$

At the beginning of the reaction, before accumulation of SNAP, the last term in eq 1 can be ignored. All the nitrogen(III) species in the reaction solution are bound by the following mass balance equation:

$$[N(III)]_T = [NO_2^-] + [HNO_2] + [RSNO] + [{}^+N{=}O] \quad (2)$$

The total N(III) species in this case would be the nitrite added to the reaction mixture. Since we expect the nitrosyl ion to be a transient reactive intermediate, its concentration can be assumed to be negligible. For initial rate measurements, concentration of product RSNO can also be ignored. We can apply a steady-state approximation on the nitrosyl ion to simplify eq 1 into measurable concentrations.

$$[NO^+] = \frac{k_2[HNO_2][H^+]}{k_{-2} + k_4[RSH]} \quad (3)$$

By using the dissociation constant of nitrous acid and the mass

balance eq 2, the initial rate law can now be rewritten as the following complex function of acid concentrations:

$$\text{rate} = \frac{\text{d[RSNO]}}{\text{d}t} = \frac{[\text{RSH}][\text{N(III)}]_T[\text{H}^+]}{K_a + [\text{H}^+]}\left(k_3 + \frac{k_2k_4[\text{H}^+]}{k_{-2} + k_4[\text{RSH}]}\right) \quad (4)$$

Equation 4 is supported by the kinetics data shown in Figures 4−6. Specifically, it predicts first-order kinetics with respect to NAP and nitrite without any saturation. It also predicts first-order kinetics in acid at low concentrations. When $[H^+]_0$ is low (approximately 0.10 mM or less) the second term in (4) becomes negligible and the reaction retains first-order kinetics on the basis of the first term only. The prevailing "free" acid concentrations have to be carefully calculated. They do not correspond to the acid added to the reaction mixture, but to the acid released by the dissociation of the weak nitrous acid added to the acid left after the strong conjugate base has sequestered as much acid as is needed to form nitrous acid. So, initial rate acid concentrations have to be calculated for each set of initial reagent concentrations. For example, an initial acid concentration of 1.0×10^{-3} M added to 2.5×10^{-3} M nitrite gives only 3.1×10^{-4} M of free acid. When initial acid concentrations are higher than nitrite, the free acid can be approximated as the excess acid over nitrite.

Evaluation of Kinetics Constants. Equation 4 has four kinetics constants that need to be evaluated. These can be reduced to three if the equilibrium constant for reaction R8 (K_2) is known with certainty for these experimental conditions. Since reactions R9 and R10 are the rate-determining steps, an initial approximation would be that $k_{-2} \gg k_4$. This would simplify eq 4 to read:

$$\frac{\text{d[RSNO]}}{\text{d}t} = \frac{[\text{RSH}][\text{N(III)}]_T[\text{H}^+]}{K_a + [\text{H}^+]}(k_3 + K_2k_4[\text{H}^+]) \quad (5)$$

A series of three NAP-dependence experiments were performed at different acid concentrations. To simplify the calculation for acid concentrations, $[H^+]_0 = [NO_2^-]_0$ so that acid concentrations could be calculated from the dissociation of HNO_2 without any contribution from the protons derived from excess acid. Plots of the reactant $[RSH]_0$ vs initial rates gave linear plots which were utilized to evaluate the bimolecular rate constant k_3. The slope of this plot was $\{[N(III)]_T[H^+]/K_a + [H^+]\}(k_3 + K_2k_4[H^+])$. For these calculations, K_a for nitrous acid was taken to be 5.62×10^{-4} M. These three plots are shown in Figure 8. Only two NAP dependence series of initial rate data were required, but in this case, a third set was produced to check the validity of the other two. The algebraic form of the slope was intractable with respect to an independent evaluation of K_2 and k_4, and instead could only provide the product of these two constants. Figure 8 was first plotted without weighting the origin, and when the plots gave an intercept kinetically indistinguishable from zero, the plots were then re-done while utilizing the origin as a data point. The data in Figure 8 provided a bimolecular rate constant for the direct reaction of NAP and HNO_2 of 2.69 M^{-1} s^{-1}. The product K_2k_4 was evaluated from the same data as 3.15×10^3 M^{-2} s^{-1}. A number of papers have studied reaction R9, but none have given a reliable value of the equilibrium constant, K_2, and so an accurate evaluation of k_4 is not possible.

Mechanistic Basis of the Effect of Cu(I) Ions. Recent studies using density functional theory[40,41] have reported that

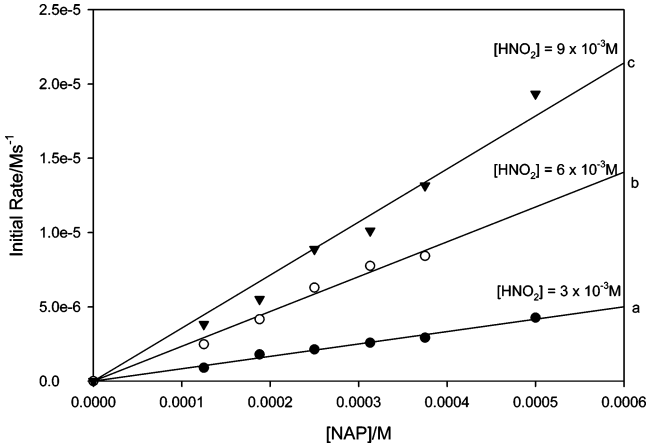

Figure 8. Combined NAP dependence plots at three different nitrous acid concentrations. The traces are labeled with the appropriate nitrous acid concentrations. The only variable was NAP concentration. These data were utilized in eq 4 for the evaluation of $k_3 = 2.69 \pm 0.33$ M^{-1} s^{-1}.

Cu^+ ions can bind to the S and N centers of nitrosothiols but that, for the model compound HSN═O, the binding to the S atom is 39.6 kJ more stable than binding to the N atom. The binding to the S atom also lengthens and weakens the S−N bond while concomitantly shortening and strengthening the N═O bond. This results in the increase in the decomposition of nitrosothiols to release NO. This increase in the lability of nitrosothiols in the presence of copper ions could be the mechanism obtained in the physiological environment for the biochemical regulation of NO release from nitrosothiols in the presence of some metalloenzymes. Our data in Figure 7A,B clearly show that stoichiometric amounts of SNAP are not obtained in the presence of Cu^+ ions. Some previous research workers had noted that both Cu(II) and Cu(I) accelerate the decomposition of nitrosothiols through a homolytic cleavage of the C−S bond to yield disulfides and nitric oxide[42] (reaction R2). The effect of Cu(II) was assumed to involve its initial reduction to Cu(I), which is the more active ion. This reduction can be accomplished by the thiolate ions that exist in thiol solutions[43]

$$2RS^- + 2Cu^{2+} \rightarrow RSSR + 2Cu^+ \quad \text{(R11)}$$

$$RSNO + Cu^+ \rightleftharpoons X^+ \rightarrow RSSR + NO + Cu^+ \text{ (unbalanced)} \quad \text{(R12)}$$

where X^+ is the complex with the copper ion attached to the nucleophilic sulfur center. The acidic conditions utilized in our experiments preclude the significant formation of thiolate ions resulting in the inertness of Cu^{2+} in this reaction mixture. Work reported in ref 41 (Askew et al) was performed at the physiological pH 7.4, which can explain the possibility of forming thiolate anions. If reaction R11 is not viable, then there is no possibility of Cu^{2+}/Cu^+ redox cycling as has been suggested by other workers.[44] The data in Figure 7C show that Cu(II) is an inert ion and does not influence the decomposition of nitric oxide. The reaction rates are invariant under a change of $[Cu(II)]_0$. The observed changes in the absorbances for the different Cu(II) concentrations are derived from the contribution the Cu(II) compound makes to the absorbance at 339 nm.

Calculations. The formation of SNAP is a very simple 4-reaction mechanism with two rate-determining steps and very few unknown kinetics variables. The simulations were undertaken only to enable us to evaluate the bimolecular rate constant

TABLE 1: Reaction Scheme and Kinetics Constants Used in Modeling the NAP−HNO_2 Reaction

reaction no.	reaction	forward rate constant, $M^{-1}\,s^{-1}$	reverse rate constant, $M^{-1}\,s^{-1}$
R7	$H^+ + NO_2^- \rightleftharpoons HNO_2$	1.1×10^9	6.18×10^5
R8	$HNO_2 + H^+ \rightleftharpoons {}^+N{=}O + H_2O$	3.16×10^5	1.00×10^7
R9	$RSH + HNO_2 \rightarrow RSNO + H_2O$	2.69	ca. 0
R10	$RSH + {}^+N{=}O \rightleftharpoons RSNO + H^+$	3.00×10^4	1.00×10^{-3}

for reaction R9, k_4. The value adopted was based on the best fit and the value reported in the literature for K_2. Table 1 shows the mechanism utilized in the calculations as well as the adopted rate constants.

Reaction R7. This is a rapid protolytic reaction that should be fast in both directions. The ratio of the forward and reverse rate constants for this equilibrium is constrained to the acid dissociation constant of nitrous acid, K_a. Once k_1 is set, then k_{-1} is also automatically set. The simulations were insensitive to the values for the kinetics constants adopted for this rapid protolytic reaction as long as they were faster than any other reaction in the reaction mixture and they adhered to the value of the acid dissociation constant, K_a.

Reaction R8. Several research groups have studied this reaction, but no one has been able to assign a reliable value to the equilibrium constant.[39,45] It is normally written as:

$$HONO + H_3O^+ \rightleftharpoons H_2ONO^+ + H_2O \qquad (R13)$$

The most recent work reported on this equilibrium established a pK_a value of 1.5 but quickly added that the pK_a value has no real thermodynamic significance apart from the fact that it fit in their numerical modeling studies of the experimental deviation of their calculated pK_a for nitrous acid in pH conditions less than 2.7. For our calculations, then, we used an initial guess of K_2 as 3.162×10^{-2} M^{-1}. Thus we expect the nitrosyl ion concentrations to be negligible in pH conditions above 3.0. In this pH range, the reaction proceeds predominantly through reaction R9.

Reaction R9. The bimolecular rate constant for this reaction was derived in this study and was fixed at that value for all calculations. It was assumed to be irreversible.

Reaction R10. There was no experimental technique that could be used to isolate this reaction for the evaluation of an upper-limit rate constant value. The value of k_4K_2 evaluated from experimental data was only used to estimate an initial guess. The final adopted value of 3.00×10^4 M^{-1} s^{-1} was derived from the best fit. The reverse rate constant was important in highly acidic conditions where the decomposition of RSNO was much faster.

Reaction R2. This is the general decomposition reaction of RSNO that proceeds at a much slower pace than the formation of RSNO. Without Cu(I) ions, this reaction did not interfere with the kinetics of formation of RSNO.

Computational Results. The fitting of the data was simple and the best fit value was obtained with $k_4 = 3.00 \times 10^4$ M^{-1} s^{-1} and $k_3 = 2.69$ M^{-1} s^{-1}. Figure 9 shows a comparison between experimental and calculated RSNO formation kinetics. The fit is adequate for such a simple model. Figure 9 shows that the model can satisfactorily reproduce the NAP dependence of the reaction rate. The value of $k_{-4} = 0.001$ M^{-1} s^{-1} was sufficient to simulate the dissociation observed in high acid conditions of Figure 6A. The adopted value for k_4 was heavily dependent on the adopted value of K_2 from ref 45, and would most likely not be valid in physiological conditions of pH 7.4.

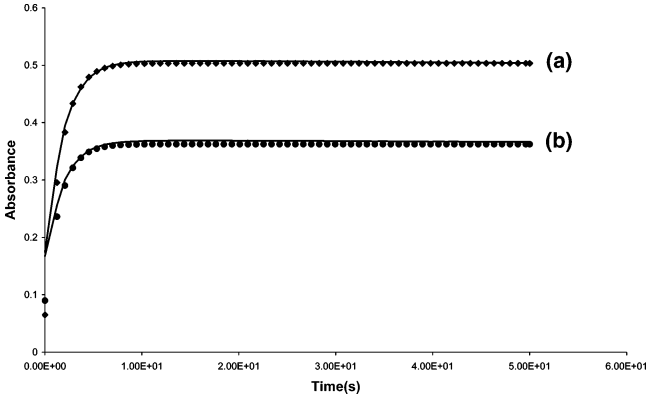

Figure 9. Calculations based on mechanism and kinetics constants in Table 1 for the NAP dependence shown in Figure 4C. Plots for (a) (−) experimental and (◆) simulated for 5×10^{-4} M NAP + 5×10^{-3} M NO_2^- + 0.1M H^+ and (b) (−) experimental and (●) simulated for 3.125×10^{-4} M NAP + 5×10^{-3} M NO_2^- + 0.1 M H^+.

Conclusion

This paper has shown that the nitrosation of NAP is accomplished through the direct reaction of nitrous acid with NAP as well as through the formation of the nitrosyl ion, which acts as the nitrosation agent. The nitrosyl ion is abundant only in highly acidic environments, but above pH 3.00 nitrosation is predominantly through nitrous acid.

Acknowledgment. We would like to acknowledge our research collaborator, Paul Siegel, for allowing us the use of the TOF mass spectrometer at the Health Effects Laboratory of the National Institute of Occupational Safety and Health based in Morgantown, West Virginia. This work was supported by research grant nos. CHE 0341769 and CHE 0137435 from the National Science Foundation.

References and Notes

(1) Marletta, M. A. *J. Biol. Chem.* **1993**, *268*, 12231−12234.
(2) Kiris, T.; Karasu, A.; Yavuz, C.; Erdem, T.; Unal, F.; Hepgul, K.; Baloglu, H. *Acta Neurochir.* **1999**, *141*, 1323−1329.
(3) Lau, H. K. F. *Atherosclerosis* **2003**, *166*, 223−232.
(4) Murata, J. I.; Tada, M.; Iggo, R. D.; Sawamura, Y.; Shinohe, Y.; Abe, H. *Mutat. Res.* **1997**, *379*, 211−218.
(5) Yun, H. Y.; Dawson, V. L.; Dawson, T. M. *Mol. Psychiatry* **1997**, *2*, 300−310.
(6) Gries, A.; Bottiger, B. W.; Dorsam, J.; Bauer, H.; Weimann, J.; Bode, C.; Martin, E.; Motsch, J. *Anesthesiology* **1997**, *86*, 387−393.
(7) Abramson, S. B.; Amin, A. R.; Clancy, R. M.; Attur, M. *Best Pract. Res. Clin. Rheumatol.* **2001**, *15*, 831−845.
(8) McBride, A. G.; Borutaite, V.; Brown, G. C. *Biochim. Biophys. Acta* **1999**, *1454*, 275−288.
(9) Stewart, A. G.; Phan, L. H.; Grigoriadis, G. *Microsurgery* **1994**, *15*, 693−702.
(10) Szabo, C. *Brain Res. Bull.* **1996**, *41*, 131−141.
(11) Richardson, G.; Benjamin, N. *Clin. Sci.* **2002**, *102*, 99−105.
(12) Millller, M. R.; Roseberry, M. J.; Mazzei, F. A.; Butler, A. R.; Webb, D. J.; Megson, I. L. *Eur. J. Pharmacol.* **2000**, *408*, 335−343.
(13) Smith, J. N.; Dasgupta, T. P. *Inorg. React. Mech.* **2001**, *3*, 181−195.
(14) Kocis, J. M.; Kuo, W. N.; Nibbs, J. *FASEB J.* **2003**, *17*, A191.
(15) Kuo, W. N.; Kocis, J. M.; Nibbs, J. *Front. Biosci.* **2003**, *8*, A62−A69.
(16) Scorza, G.; Pietraforte, D.; Minetti, M. *Free Radical Biol. Med.* **1997**, *22*, 633−642.
(17) Tsikas, D.; Sandmann, J.; Luessen, P.; Savva, A.; Rossa, S.; Stichtenoth, D. O.; Frolich, J. C. *Biochim. Biophys. Acta* **2001**, *1546*, 422−434.
(18) Boese, M.; Mordvintcev, P. I.; Vanin, A. F.; Busse, R.; Mulsch, A. *J. Biol. Chem.* **1995**, *270*, 29244−29249.
(19) Jourd'heuil, D.; Laroux, F. S.; Miles, A. M.; Wink, D. A.; Grisham, M. B. *Arch. Biochem. Biophys.* **1999**, *361*, 323−330.

(20) Stamler, J. S.; Jaraki, O.; Osborne, J.; Simon, D. I.; Keaney, J.; Vita, J.; Singel, D.; Valeri, C. R.; Loscalzo, J. *Proc. Natl. Acad. Sci. U.S.A.* **1992**, *89*, 7674−7677.

(21) Gaston, B.; Reilly, J.; Drazen, J. M.; Fackler, J.; Ramdev, P.; Arnelle, D.; Mullins, M. E.; Sugarbaker, D. J.; Chee, C.; Singel, D. J.; Loscalzo, J.; Stamler, J. S. *Proc. Natl. Acad. Sci. U.S.A.* **1993**, *90*, 10957−10961.

(22) Haqqani, A. S.; Do, S. K.; Birnboim, H. C. *Nitric Oxide* **2003**, *9*, 172−181.

(23) Stamler, J. S.; Toone, E. J. *Curr. Opin. Chem. Biol.* **2002**, *6*, 779−785.

(24) Wang, K.; Zhang, W.; Xian, M.; Hou, Y. C.; Chen, X. C.; Cheng, J. P.; Wang, P. G. *Curr. Med. Chem.* **2000**, *7*, 821−834.

(25) Hogg, N.; Singh, R. J.; Konorev, E.; Joseph, J.; Kalyanaraman, B. *Biochem. J.* **1997**, *323*, 477−481.

(26) Trujillo, M.; Alvarez, M. N.; Peluffo, G.; Freeman, B. A.; Radi, R. *J. Biol. Chem.* **1998**, *273*, 7828−7834.

(27) Aquart, D. V.; Dasgupta, T. P. *Biophys. Chem.* **2004**, *107*, 117−131.

(28) Ng, C. W.; Najbar-Kaszkiel, A. T.; Li, C. G. *Clin. Exptl. Pharmacol. Physiol.* **2003**, *30*, 357−361.

(29) Holder, A. A.; Marshall, S. C.; Wang, P. G.; Kwak, C. H. *Bull. Korean Chem. Soc.* **2003**, *24*, 350−356.

(30) Clancy, R.; Cederbaum, A. I.; Stoyanovsky, D. A. *J. Med. Chem.* **2001**, *44*, 2035−2038.

(31) Wink, D. A.; Cook, J. A.; Kim, S. Y.; Vodovotz, Y.; Pacelli, R.; Krishna, M. C.; Russo, A.; Mitchell, J. B.; Jourdheuil, D.; Miles, A. M.; Grisham, M. B. *J. Biol. Chem.* **1997**, *272*, 11147−11151.

(32) Hogg, N. *Annu. Rev. Pharmacol. Toxicol.* **2002**, *42*, 585−600.

(33) Aravindakumar, C. T.; De Ley, M.; Ceulemans, J. *J. Chem. Soc., Perkin Trans. 2* **2002**, 663−669.

(34) Wink, D. A.; Nims, R. W.; Darbyshire, J. F.; Christodoulou, D.; Hanbauer, I.; Cox, G. W.; Laval, F.; Laval, J.; Cook, J. A.; Krishna, M. C.; Degraff, W. G.; Mitchell, J. B. *Chem. Res. Toxicol.* **1994**, *7*, 519−525.

(35) Szacilowski, K.; Stasicka, Z. *Prog. React. Kinet. Mech.* **2001**, *26*, 1−58.

(36) Wang, K.; Zhang, W.; Xian, M.; Hou, Y. C.; Chen, X. C.; Cheng, J. P.; Wang, P. G. *Curr. Med. Chem.* **2000**, *7*, 821−834.

(37) Vasquez-Vivar, J.; Santos, A. M.; Junqueira, V. B.; Augusto, O. *Biochem. J.* **1996**, *314* (Pt 3), 869−876.

(38) Aykac-Toker, G.; Bulgurcuoglu, S.; Kocak-Toker, N. *Hum. Exp. Toxicol.* **2001**, *20*, 373−376.

(39) Beake, B. D.; Moodie, R. B. *J. Chem. Soc., Perkin Trans. 2* **1998**, 1−5.

(40) Baciu, C.; Cho, K. B.; Gauld, J. W. *Eur. J. Mass Spectrom.* **2004**, *10*, 941−948.

(41) Baciu, C.; Cho, K. B.; Gauld, J. W. *J. Phys. Chem. B* **2005**, *109*, 1334−1336.

(42) Askew, S. C.; Barnett, D. J.; Mcaninly, J.; Williams, D. L. H. *J. Chem. Soc., Perkin Trans. 2* **1995**, 741−745.

(43) Butler, A. R.; Al Sa'doni, H. H.; Megson, I. L.; Flitney, F. W. *Nitric Oxide* **1998**, *2*, 193−202.

(44) Singh, R. J.; Hogg, N.; Joseph, J.; Kalyanaraman, B. *J. Biol. Chem.* **1996**, *271*, 18596−18603.

(45) Koch, T. G.; Sodeau, J. R. *J. Phys. Chem.* **1995**, *99*, 10824−10829.